

# Non-quasi-static Effects Simulation of Microwave Circuits based on Physical Model of Semiconductor Devices

Ke Xu, Xing Chen, and Qiang Chen

College of Electronics and Information Engineering  
Sichuan University, Chengdu, Sichuan 610065, China  
xingc@live.cn

**Abstract** — This work explores analyzing the non-quasi-static effects of a microwave circuit by employing a physical model-based field-circuit co-simulation method. Specifically, it uses the semiconductor physical model to characterize the semiconductor devices, and simulates the lumped circuit by cooperating semiconductor physical equations into Kirchhoff's circuit equations. Then the lumped circuit simulation is hybridized with the finite-difference time-domain (FDTD) simulation by interfacing EM (electromagnetic) field quantities with lumped-element quantities at each timestep. Taken a microwave limiter circuit as an example, the simulation results agree well with the measured results, which prove that this method can characterize non-quasi-static effects well. As a comparison, the equivalent circuit model-based co-simulation cannot characterize the non-quasi-static effects accurately.

**Index Terms** — Full-wave simulation, non-quasi-static effects, PIN microwave limiter, semiconductor physical model.

## I. INTRODUCTION

To analyze the microwave circuit and evaluate its electromagnetic compatibility characteristics, the field-circuit co-simulation method is widely used [1]. It solves Maxwell's equations and Kirchhoff's equations simultaneously to characterize interactions between electromagnetic waves and active/passive circuit elements. In the field-circuit co-simulation method, semiconductor devices' nonlinear characteristics play an important role [2]. Especially as the operating frequency increases, the nonlinear non-quasi-static effects of semiconductor devices cannot be ignored anymore [3]. Because in the quasi-static effects, the channel charge is assumed to be equilibrium once biases are applied, thus the finite charging time of the carriers in the inversion layer is ignored [3]. This gives erroneous simulation results for signals with a working time period comparable to or smaller than the channel transit time [3]. Hence, more and more researchers aim at modeling and

simulating the non-quasi-static effects of microwave circuits [3-6].

By now, the non-quasi-static effects of microwave circuits are mainly simulated by the equivalent circuit model-based field-circuit co-simulation method [3-6]. For example, non-quasi-static models of the Tunneling FETs [4] and MOSFET [5,6] are proposed, which all belong to the equivalent circuit model. However, the equivalent circuit models still do not have enough accuracy, because the models are obtained with an approximation to the physical equations [5]. Moreover, the parameters within the models are not easy to be determined [6]. And in those cases, the physical model of semiconductor devices is of great advantage and highly desirable, which is based on the physical equations of the semiconductor devices and highly accurate [7].

Furthermore, the current studies on physical model-based simulation of circuits mainly don't involve the electromagnetic computation [8-11] or rarely explored simulating non-quasi-static effects of circuits working at high frequencies [12-15]. One of the reasons is that the complicated physical model-based simulation needs to solve not only the semiconductor physical equations but also Maxwell's equations [7]. Moreover, constructing a precise model and extracting precise physical parameters of semiconductor devices are crucial in the simulation of circuits working at high frequencies [16]; as some extracted parameters usually work well at low frequencies but badly at high frequencies. Hence, current investigations on physical simulation of circuits at high frequency don't involve electromagnetic computation, or they are limited to special self-designed semiconductor devices with known physical parameters rather commercial semiconductor devices [8-11].

Hence, this work focuses on analyzing the non-quasi-static effects of a microwave circuit by the physical model-based field-circuit co-simulation. In this method, the semiconductor physical equations are cooperated into Kirchhoff's equations to obtain node voltages and branch currents of a lumped circuit, then this circuit simulation is coupled with FDTD simulation

by interfacing quantities between them. Moreover, a commercial PIN diode limiter circuit is taken as an example, which shows strongly non-quasi-static effects, because the length of the base region is thin enough. The limiter circuit is simulated by the physical model-based field-circuit co-simulation, and the accuracy of this method in simulating non-quasi-static effects is validated by comparing it with the measured results.

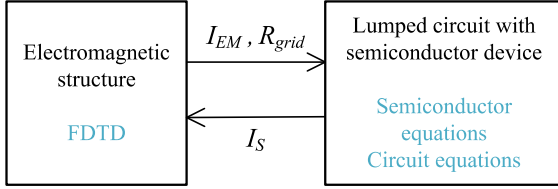


Fig. 1. The division and interfacing principle of the field-circuit hybrid system.

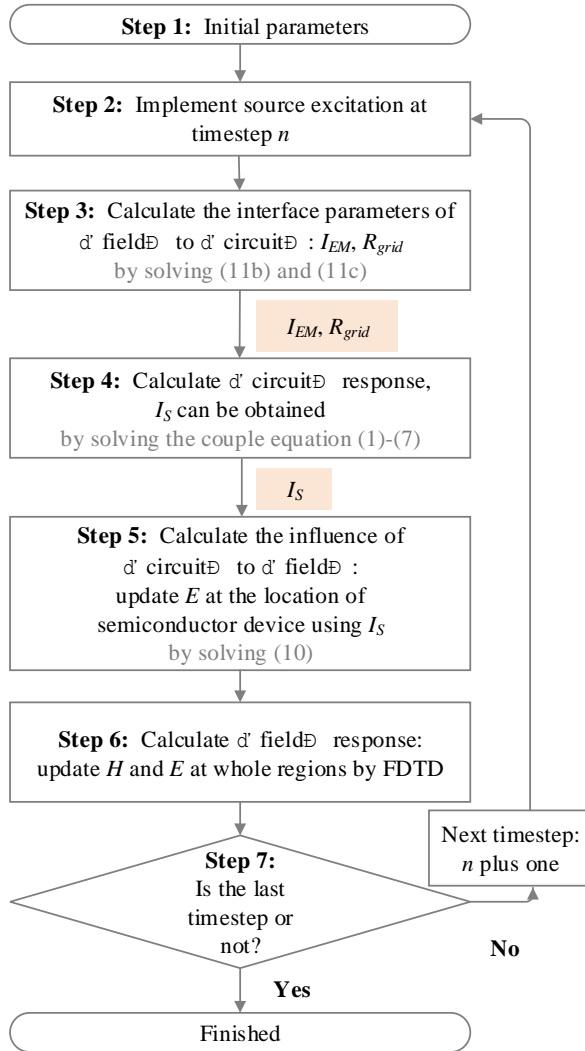


Fig. 2. The physical model-based field-circuit co-simulation procedure.

## II. SIMULATION METHOD

In the co-simulation method, the field-circuit hybrid system is divided into two parts [17]: (1) the distributed electromagnetic structure, which is characterized by Maxwell's equations; (2) the lumped circuit comprising with semiconductor devices, which is characterized by semiconductor equations and Kirchhoff's equations. The two parts are coupled by interfacing lumped circuit quantities  $U$  and  $I$ , with electromagnetic-field quantities  $E$  and  $H$ , as shown in Fig. 1.

The simulation flowchart is shown in Fig. 2. At each timestep, after implementing source excitation, the key four steps are step 3-6: Step 4 and 6 calculate "circuit" and "field" response, respectively; step 3 and step 5 calculate the interface parameters  $I_{EM}$ ,  $R_{grid}$  and  $I_S$  between the "field" and "circuit" parts. After these steps, it will march to the next timestep. These key steps will be introduced as follows.

### A. Step 4: The physical model-based lumped circuit simulation

The lumped circuit is solved by using Kirchhoff's current equation. In a lumped circuit, assume that a lumped element is located between  $(k-1)^{th}$  and  $k^{th}$  node, the relationship between its current  $I_j$  and node voltage  $U_k$  and  $U_{k-1}$  is described in (1). According to the Kirchhoff's current equation [17], the sum of all currents leaving a node is zero, as (2):

$$I_j = \psi(U_k, U_{k-1}), \quad (1)$$

$$\sum I_j = 0. \quad (2)$$

After substituting (1) to (2), (2) is solved by the Newton-Raphson iteration method [17]. Hence, the transient voltage and current of the lumped circuit can be obtained.

For a lumped circuit element, such as a resistor or a capacitance, the relationship described in (1) can be obtained by analytic equations.

For a specific semiconductor device, it is modeled by the drift-diffusion physical model, which can characterize the non-quasi-static effects well, as the equation group (3-7) [18]:

$$\mathbf{J}_n = qD_n \nabla n_e - q\mu_n n_e \nabla \varphi, \quad (3)$$

$$\mathbf{J}_p = -qD_p \nabla p - q\mu_p p \nabla \varphi, \quad (4)$$

$$\partial n_e / \partial t = q^{-1} \nabla \cdot \mathbf{J}_n + G - R, \quad (5)$$

$$\partial p / \partial t = -q^{-1} \nabla \cdot \mathbf{J}_p + G - R, \quad (6)$$

$$\nabla \cdot (\epsilon_s \nabla \varphi) = q(n_e - p + N_A - N_D). \quad (7)$$

Equation (3) and (4) are current equations for electrons and holes in a semiconductor, equation (5) and (6) are continuity equations for electron and hole, equation (7) is Poisson's equation, where  $J_n$  and  $J_p$  are the electron and hole current densities,  $q$  is the electronic charge,  $D_n$  and  $D_p$  are the hole and electron diffusion coefficients,  $n_e$  and  $p$  are the electron and hole density respectively,  $\mu_n$  and  $\mu_p$  are the hole and electron mobility

respectively,  $\phi$  is the electric potential,  $t$  is time,  $\epsilon_s$  is the permittivity of the semiconductor material,  $R$  is electron-hole recombination rate,  $G$  is electron-hole generation rate,  $N_A$  is acceptor impurity concentration, and  $N_D$  is donor impurity concentration.

Discrete (3-7) on the mesh of the semiconductor device chip's 1D physical model, and solve the discrete equations in time domain by the finite difference method [19], the relationship between voltage and current of the semiconductor device can be obtained.

In conclusion, the characteristics of the lumped circuit comprising with semiconductor devices can be obtained by solving the coupled equations (1-7).

### B. Step 6: The FDTD method

In the filed-circuit co-simulation method, the electromagnetic structure part is simulated by Maxwell's equations (8-9) by the FDTD method [20]:

$$\nabla \times \mathbf{E} = -\mu \frac{\partial \mathbf{H}}{\partial t}, \quad (8)$$

$$\nabla \times \mathbf{H} = \mathbf{J} + \epsilon \frac{\partial \mathbf{E}}{\partial t}, \quad (9)$$

where  $\mathbf{E}$  is the electric field,  $\mathbf{H}$  is the magnetic intensity,  $\epsilon$  is the permittivity,  $\mu$  is the permeability,  $\mathbf{J}$  is the current density.

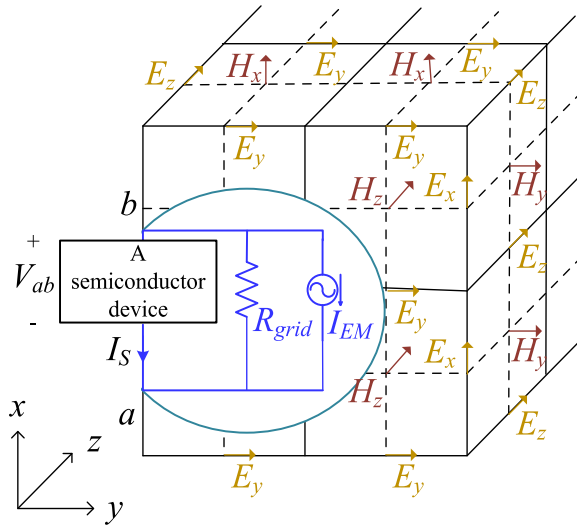


Fig. 3. A semiconductor device is located on the Yee grid of a distributed electromagnetic structure.

### C. Step 3, 5: The field-circuit interfacing method

At the location where the semiconductor device is located, the electric field  $\mathbf{E}$  and magnetic intensity  $\mathbf{H}$  need to be specially treated to interface "field" and "circuit" parts, which is shown as follows.

Assume that a semiconductor device is located along the  $x$ -axis from  $a$  point to  $b$  point on the Yee grid,

as shown in Fig. 3. The current through the semiconductor device is  $I_s$ . On the Yee grid from  $a$  point to  $b$  point, we assume that the permittivity  $\epsilon$  and mesh are uniform for simplicity, equation (9a) can be discretized to (10a) [17], the discretization can also be generalized to the ununiform situation:

$$E_{x(i+\frac{1}{2},j,k)}^{n+1} = K_{xijk}^{n+1} - \Gamma_{xijk}^{n+1} \cdot I_{sx}^{n+1}, \quad (10a)$$

where

$$\Gamma_{xijk}^{n+1} = \frac{dt}{\epsilon dy dz}, \quad (10b)$$

$$K_{xijk}^{n+1} = E_{x(i+\frac{1}{2},j,k)}^n + \Gamma_{xijk}^{n+1} \cdot [ (H_{z(i+\frac{1}{2},j+\frac{1}{2},k)}^{n+\frac{1}{2}} - H_{z(i+\frac{1}{2},j-\frac{1}{2},k)}^{n+\frac{1}{2}}) \cdot dz - (H_{y(i+\frac{1}{2},j,k+\frac{1}{2})}^{n+\frac{1}{2}} - H_{y(i+\frac{1}{2},j,k-\frac{1}{2})}^{n+\frac{1}{2}}) \cdot dy ] \quad (10c)$$

where  $\Gamma$  and  $K$  are intermediate variables, the subscript index  $i, j, k$  indicate the location on Yee grid at  $x, y, z$  direction, respectively; the superscript index  $n$  indicates the timestep;  $dx, dy,$  and  $dz$  are cell sizes at corresponding directions.

Assume that the voltage across the semiconductor device is  $V_{ab}$ , which can be obtained by integrating the electric field from  $a$  point to  $b$  point, hence (10a) is integrated to (11a) [17]:

$$V_{ab}^{n+1} = [(I_x^{n+1})_{EM} - I_{sx}^{n+1}] (R_x^{n+1})_{grid}, \quad (11a)$$

where

$$(R_x^{n+1})_{grid} = \sum_{(i_a, j_a, k_a)}^{(i_b, j_b, k_b)} \Gamma_{xijk}^{n+1} dx, \quad (11b)$$

$$(I_x^{n+1})_{EM} = \frac{\sum_{(i_a, j_a, k_a)}^{(i_b, j_b, k_b)} K_{xijk}^{n+1} dx}{(R_x^{n+1})_{grid}}. \quad (11c)$$

In (11a),  $I_{EM}$ ,  $R_{grid}$ , and  $I_s$  can equivalently form a parallel lumped circuit, as shown in Fig. 3. By this equivalent circuit, the "field" and "circuit" parts are interfaced. In this parallel circuit,  $I_s$  is the current through the semiconductor device;  $I_{EM}$  and  $R_{grid}$  are equivalent circuit model of the distributed electromagnetic structure at timestep  $(n+1)$ .

Hence in the flowchart,  $I_{EM}$  and  $R_{grid}$  are calculated by (11a) and (11b) in step 3, which characterize the effect of the "field" to "circuit". Then they are passed to step 4, the formed parallel circuit is calculated by the physical model-based lumped circuit simulation, and the current through the semiconductor device  $I_s$  can be obtained.  $I_s$  characterizes the influence of the "circuit" to "field"; then in step 5, the electric field is updated by (10a) using  $I_s$  at the location where the semiconductor device is located [17]. In this way, the physical-model circuit simulation and FDTD field simulation are integrated into a unified scheme.

### III. RESULTS

To verify the feasibility and accuracy of this simulation method in simulating the non-quasi-static effects of a microwave circuit, a microwave limiter circuit is taken as an example and simulated.

A commercial PIN diode SMP1330 is selected as the limiter diode, because this diode shows strongly non-quasi-static effects at microwave frequencies. The length of this PIN diode base region  $X_B = 2 \text{ }\mu\text{m}$  [21], and its transit time frequency  $f_T$  is about 325 MHz. The transit time frequency  $f_T$  of a PIN diode in megahertz can be calculated by (12) [22]:

$$f_T \approx \frac{1300}{X_B^2}. \quad (12)$$

The working frequency range of the limiter is 0.5-2.5 GHz, which is higher than the transit time frequency, and the non-quasi-static effects dominate its electric characteristics [23].

#### A. Simulation model

The configuration of the limiter circuit is in Fig. 4. The limiter diode is connected between the center of microstrip and a grounding via. The left and right end of the microstrip is input port 1 and output port 2, respectively.

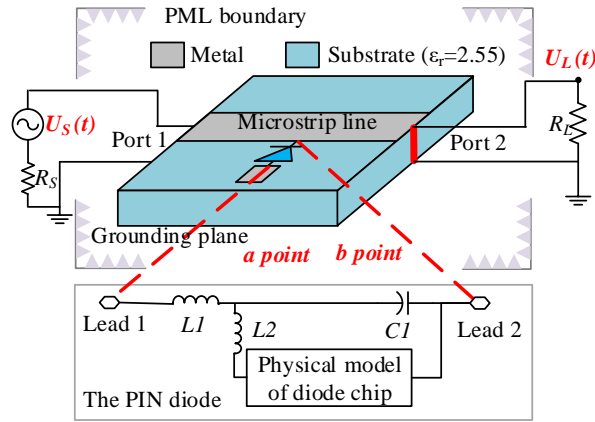


Fig. 4. The configuration and simulation model of the PIN limiter circuit.

The simulation model is also shown in Fig. 4, the main issues arising with the modeling will be explained:

1) The model is divided into two parts: the electromagnetic structure which is within the PML boundary and the lumped circuit which is within the grey solid rectangle.

2) Source and load. The discrete Thévenin source is added to port 1 to characterize the signal source, it consists of a time-varying voltage source  $U_S(t)$  and an input resistance  $R_S$  of 50 ohms. Moreover, a lumped load resistance  $R_L$  of 50 ohms is added to port 2 to characterize the load. The voltage across  $R_L$  is  $U_L(t)$ .

3) The simulation model of the PIN diode is comprised of two parts: the physical model of chip and the equivalent circuit model of the semiconductor package. The physical model of the diode chip is characterized by its doping profile, which can be obtained from the physical parameters of the chip [24]. A GA-based curve fitting approach is applied to extract the physical parameters from the measurement results, and its doping profile is shown in Fig. 5.

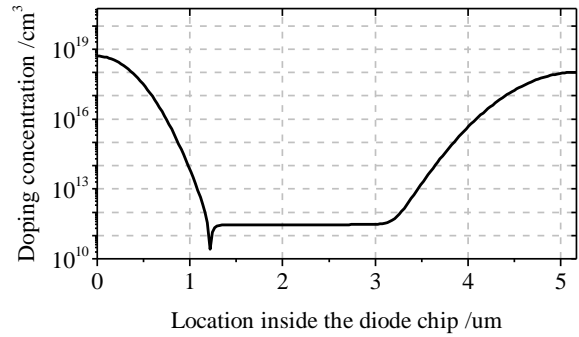


Fig. 5. The doping concentration profile of the diode chip physical model.

Using the simulation model described above, the limiter circuit is simulated by the physical model-based field-circuit co-simulation method.

To compute the scattering parameters of the limiter, a unit amplitude modulated Gaussian pulse is injected to the input port 1 as excitation, the reflection waveform at input port 1, and transmitter voltage waveform at output port 2 are calculated to obtain S11 and S21 respectively.

The output power vs input power curve of the limiter can be calculated. The input signal  $U_S(t)$  is defined as a sine wave with an amplitude of  $A$  at working frequency  $f$ , as in (13). Hence the input power can be obtained, as in (14):

$$U_S = A \cdot \sin(2\pi f), \quad (13)$$

$$P_{input} = 0.125 \cdot A^2 / R_S. \quad (14)$$

The output power defines as the power that is being consumed on the load  $R_L$ , which presents the power “delivered to” the following circuit connected to the limiter. The output voltage waveform  $U_L(t)$  can be calculated by the physical-model simulation method, hence the output power can be calculated by integrating transient power over a time period:

$$P_{output} = \int_{t=0}^{t=T} \frac{U_L(t)^2}{R_L} dt. \quad (15)$$

By calculating the relationship between input power and output power with the input power increases, the output power vs input power curve can be obtained.

#### B. Measure method

Figure 6 shows the measure setup of the output

power vs input power curve. By coaxial lines and SMA connectors, the two ports are connected to signal source and power meter respectively. The signal source is characterized by the voltage source  $U_S(t)$  and internal resistance  $R_S$ ; the power meter is characterized by the load resistance  $R_L$  in the simulation model of Fig. 4. The displayed output power of the signal source is the input power of the limiter, the displayed input power of the power meter is the output power of the limiter. Hence, the output power vs input power curve can be measured.

The measured output power vs input power curve is shown in Fig. 8. It can be observed that, the output power is equal to input power when the input power is less than 7 dBm, which means that there is no attenuation at this input power range. However, with the input power increases, the output power attenuation increases. There is nearly 8.99 dB attenuation when the input power is 23 dBm, which means that 87.38% of the input power is reflected to the signal source. Because the impedance of the limiter diode is small due to the non-quasi-static effects when the large signal inputs [23].

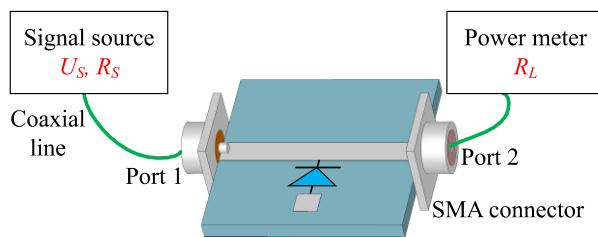


Fig. 6. The measure setup of the output power vs input power curve.

### C. Simulation results

The simulated and measured scattering parameters of the limiter are shown in Fig. 7. From the figure, the physical model-based field-circuit co-simulation method can characterize the small-signal scattering parameters well. There is hardly any loss at 500 MHz; but the loss increases with the working frequency increasing, and the S11 is 0.5 dB at 2.5 GHz. The loss generates from both the microstrip structure and the diode itself.

The simulated and measured power limiting characteristics, namely the output power vs input power curve at 1 GHz is shown in Fig. 8. As mentioned above, this power characteristic is dominated by the non-quasi-static effects. As shown in the figure, the simulated results agree well with the measured results. The output power is equal to the input power when the input power is less than 7 dBm. Both the simulated and measured results show that the 1dB compression point is 8 dBm. The measured attenuation of the output power is nearly 8.99 dB when the input power is 23 dBm; the simulated attenuation is 9.11 dB, which means the simulation results are accurate. Meanwhile, it means that the limiter

begins to limit the output power when the input power is large enough. Moreover, from the results of Fig. 8, the limiter shows non-linear effects with the power increases. To analyze it more clearly, the output voltage waveforms  $U_L(t)$  are simulated when the input power is 4 dBm, 10 dBm, 16 dBm, and 22 dBm respectively, as shown in Fig. 9. At the four input power, the amplitude  $A$  of the input voltage  $U_S(t)$  is 1 V, 2 V, 4 V, and 8 V, which increase doubly. However, the maximum output voltage value of  $U_L(t)$  at the four power is 0.49 V, 0.69V, 0.95 V, and 1.33 V respectively, which do not increase doubly. The increased percentage than the previous one is 41%, 38%, and 40% respectively. It demonstrates the decrease of the limiter impedance, which is due to the accumulated carriers in the base of the diode [23], namely the non-linear non-quasi-static effects dominate the phenomenon.

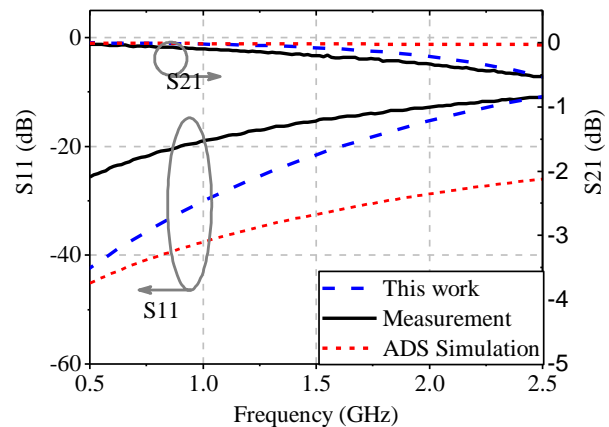


Fig. 7. The scattering parameters of the limiter.

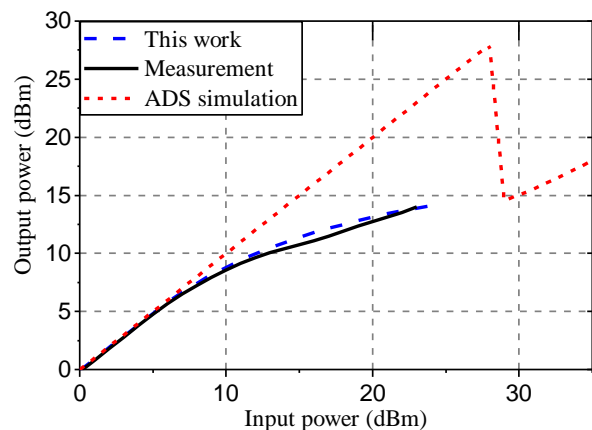


Fig. 8. The output power vs input power curve at 1 GHz of the limiter circuit.

The power limiting characteristic is also simulated by ADS using the equivalent circuit model, which is provided by the semiconductor manufacturer [21]. The results are also shown in Fig. 8. It is obvious that there

is a large divergence between the measured results and the equivalent circuit simulation results. The reason is that the inaccuracy of the equivalent circuit model in characterizing the non-quasi-static effects of the semiconductor device.

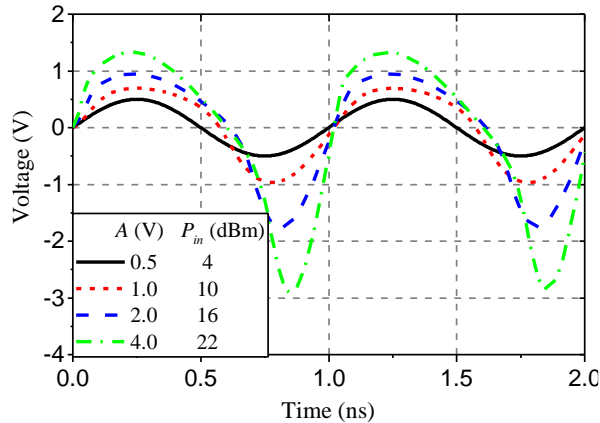


Fig. 9. The output voltage waveforms at different input power of 1 GHz.

## VI. CONCLUSION

The non-quasi-static effects of the microwave circuits are analyzed by the physical model-based simulation method. In this method, the semiconductor physical equations are cooperated into the Kirchhoff's circuit equations to obtain voltages and currents of a lumped circuit, then this circuit simulation is coupled with FDTD simulation by interfacing quantities between them.

The results show that, the simulation method in this work is largely more accurate compared with the equivalent circuit model-based simulation method. This simulation method is an attractive candidate in the simulating and predicting non-quasi-static effects of the microwave circuits.

## ACKNOWLEDGMENT

This work was supported by the Fund of Ministry of Education of China under Grant 6141A0202504.

## REFERENCES

- [1] S. Chen, D. Ding, Z. Fan, and R. Chen, "Nonlinear analysis of microwave limiter using field-circuit coupling algorithm based on time-domain volume-surface integral method," *IEEE Microwave and Wireless Components Letters*, vol. 27, no. 10, pp. 864-866, Oct. 2017.
- [2] K. ElMahgoub and A. Z. Elsherbeni, "FDTD implementations of integrated dependent sources in full-wave electromagnetic simulations," *Applied Computational Electromagnetics Society Journal*, vol. 29, no. 12, 2014.
- [3] M. Chan, K. Y. Hui, C. Hu, and P. K. Ko, "A robust and physical BSIM3 non-quasi-static transient and AC small-signal model for circuit simulation," *IEEE Transactions on Electron Devices*, vol. 45, no. 4, pp. 834-841, Apr. 1998.
- [4] B. Lu, Z. Lv, H. Lu, and Y. Cui, "A non-quasi-static model for tunneling FETs based on the relaxation time approximation," *IEEE Electron Device Letters*, vol. 40, no. 12, pp. 1996-1999, Dec. 2019.
- [5] H. Wang, T. Chen, and G. Gildenblat, "Quasi-static and nonquasi-static compact MOSFET models based on symmetric linearization of the bulk and inversion charges," *IEEE Transactions on Electron Devices*, vol. 50, no. 11, pp. 2262-2272, Nov. 2003.
- [6] Y. Cao, W. Zhang, J. Fu, Q. Wang, L. Liu, and A. Guo, "A complete small-signal MOSFET model and parameter extraction technique for millimeter wave applications," *IEEE Journal of the Electron Devices Society*, vol. 7, pp. 398-403, 2019.
- [7] F. Filicori, G. Vannini, and V. A. Monaco, "A nonlinear integral model of electron devices for HB circuit analysis," *IEEE Transactions on Microwave Theory and Techniques*, vol. 40, no. 7, pp. 1456-1465, July 1992.
- [8] J. Grajal, V. Krozer, E. Gonzalez, F. Maldonado, and J. Gismero, "Modeling and design aspects of millimeter-wave and submillimeter-wave Schottky diode varactor frequency multipliers," *IEEE Transactions on Microwave Theory and Techniques*, vol. 48, no. 4, pp. 700-711, Apr. 2000.
- [9] D. B. Ameen and G. B. Tait, "Convolution-based global simulation technique for millimeter-wave photodetector and photomixer circuits," in *IEEE Transactions on Microwave Theory and Techniques*, vol. 50, no. 10, pp. 2253-2258, Oct. 2002.
- [10] D. Pardo, J. Grajal, C. G. Pérez-Moreno, and S. Pérez, "An assessment of available models for the design of Schottky-based multipliers up to THz frequencies," *IEEE Transactions on Terahertz Science and Technology*, vol. 4, no. 2, pp. 277-287, Mar. 2014.
- [11] J. V. Siles and J. Grajal, "Physics-based design and optimization of Schottky diode frequency multipliers for Terahertz applications," *IEEE Transactions on Microwave Theory and Techniques*, vol. 58, no. 7, pp. 1933-1942, July 2010.
- [12] X. Chen, J. Q. Chen, K. Huang, and X. B. Xu, "A circuit simulation method based on physical approach for the analysis of Mot\_bal99lt1 p-i-n diode circuits," *IEEE Trans. Electron. Devices*, vol. 58, no. 9, pp. 2862-2870, Sept. 2011.
- [13] A. Subbiah and O. Wasynczuk, "Computationally efficient simulation of high-frequency transients in power electronic circuits," *IEEE Transactions on Power Electronics*, vol. 31, no. 9, pp. 6351-6361,

- Sept. 2016.
- [14] B. Allard, H. Garrab, T. B. Ben Salah, H. Morel, K. Ammous, and K. Besbes, "On the role of the N–N+ junction doping profile of a PIN diode on its turn-off transient behavior," *IEEE Transactions on Power Electronics*, vol. 23, no. 1, pp. 491–494, Jan. 2008.
- [15] A. T. Bryant, X. Kang, E. Santi, P. R. Palmer, and J. L. Hudgins, "Two-step parameter extraction procedure with formal optimization for physics-based circuit simulator IGBT and p-i-n diode models," *IEEE Transactions on Power Electronics*, vol. 21, no. 2, pp. 295–309, Mar. 2006.
- [16] T. Ren, Y. Zhang, and Z. Jin, "A 340–400 GHz zero-biased waveguide detector using an self-consistent method to extract the parameters of Schottky barrier diode," *Applied Computational Electromagnetics Society Journal*, vol. 30, no. 12, 2015.
- [17] W. Sui, *Time-Domain Computer Analysis of Non-linear Hybrid Systems*. CRC Press, 2018.
- [18] S. M. Sze and K. K. Ng, *Physics of Semiconductor Devices*. Hoboken, NJ: John Wiley & Sons, 2006.
- [19] S. Selberherr, *Analysis and Simulation of Semiconductor Devices*. Springer Science & Business Media, 2012.
- [20] A. Taflove, "A perspective on the 40-year history of FDTD computational electrodynamics," *Applied Computational Electromagnetics Society Journal*, vol. 22, no. 1, 2007.
- [21] Skyworks Solutions, Inc. "SMP1330 Series: Plastic Packaged Limiter Diodes," 2016.
- [22] J. F. White, *Microwave Semiconductor Engineering*. Van Nostrand Reinhold Company, New York, 1982.
- [23] M. E. Clarke and S. Rahim, "A non quasi-static empirical model of the power PIN diode for circuit simulation," *The International Journal for Computation and Mathematics in Electrical and Electronic Engineering*, 1994.
- [24] M. Kurata, "Design considerations of step recovery diodes with the aid of numerical large-signal analysis," *IEEE Transactions on Electron Devices*, vol. 19, no. 11, pp. 1207–1215, Nov. 1972.



**Ke Xu** received the B.S. degree in Electronics and Information Engineering from Sichuan University, Chengdu, China, in 2013. She is currently pursuing the Ph.D. degree in Radio Physics at the same university. Her research interests include computational electromagnetics and semiconductor device numerical simulation.



**Xing Chen** received the M.S. degree in Radio Physics and the Ph.D. degree in Biomedical Engineering from Sichuan University, Sichuan, China, in 1999 and 2004, respectively. In 1991, he joined as a Teaching Staff and is currently a Professor with the College of Electronics and Information Engineering, Sichuan University. His research interests include antenna, microwave imaging, global optimization, numerical methods applied in electromagnetics, and parallel computation. Chen is a Senior Member of the Chinese Institute of Electronics.



**Qiang Chen** Provide received the B.S. degree in Electronic Information Engineering and the M.S. degree in Radio Physics from Sichuan University, Sichuan, China, in 2014 and 2017, respectively. He is currently pursuing the Ph.D. degree in Radio Physics at Sichuan University. His research interests include antenna design, multi-physics computation and microwave rectifier design.